

# A Model for Diffraction-Limited High-Power Multimode Fiber Amplifiers Using Seeded Stimulated Brillouin Scattering Phase Conjugation

Gerald T. Moore

**Abstract**—Diffraction-limited polarized stimulated Brillouin scattering (SBS) Stokes output from a multimode fiber is possible when the Stokes beam is the phase conjugate of diffraction-limited polarized pump light from a narrow-band master oscillator. Net amplification can be obtained by interposing a gain medium, such as a fiber amplifier, between the master oscillator and the region of SBS generation. This paper proposes and studies numerically a model which describes the space-time dynamics of SBS generation, including phase conjugation, attenuation, phonon decay, thermal noise, inhomogeneous broadening, and amplifier gain. Noise reduction and phase locking are obtained by seeding the low-power end of the fiber at the Stokes frequency. Simulations are described for the case of 1.064  $\mu\text{m}$  light amplification in a dual-clad Yb-doped multimode fiber amplifier.

**Index Terms**—Fiber amplifiers, multimode fibers, phase conjugation, stimulated Brillouin scattering.

## I. INTRODUCTION

THE GENERATION of a backward-traveling Stokes wave by stimulated Brillouin scattering (SBS) phase conjugation (PC) in multimode fiber was studied recently [1] as a means to obtain a diffraction-limited polarized (DLP) beam from a CW Nd : YAG master oscillator/power amplifier. The oscillator linewidth was about 40 kHz. Double passage of the phase-conjugated Stokes wave back through the amplifier removed the aberrations and depolarization produced in the incident signal on the first two passages through the amplifier. The fiber had a 50  $\mu\text{m}$  core diameter and a length  $L = 3.6$  km, and the SBS reflectivity was 30% for a 1-W power input to the fiber. Reflectivity as high as 88% has been obtained by Eichler *et al.* [2], [24] using 30-ns pulses.

Discussed here are the possibilities for scaling to high power by replacing the Nd : YAG amplifier used in the above work [1] by a CW multimode Yb-core fiber amplifier. The master oscillator must produce light with a narrow frequency bandwidth (a few megahertz or less). Such light could be generated using a low-power Nd : YAG laser. This is referred to as *pump light*, not to be confused with the diode light which pumps the fiber amplifier. Both the pump light and the counter-propagating Stokes

light are amplified by the gain medium. The conditions under which it may be possible to control the phase of the Stokes output of such an amplifier by injection-seeding the opposite end of the fiber at the Stokes frequency are discussed. Injection locking an array of fiber amplifiers to a common seed is an important step toward coherent combination of their outputs. One way to generate a suitable Stokes seed is by down-shifting a portion of the Nd : YAG radiation in a low-power single-mode Brillouin–Yb fiber laser. This would operate similarly to a Brillouin–Er fiber laser [3], and provide a stable Stokes shift even if the Nd : YAG laser drifted in frequency.

A multimode fiber amplifier using SBS PC has several potential advantages over single-mode Yb-doped fiber lasers. The latter, especially at high power, commonly produce unpolarized output with a wide bandwidth (hundreds of gigahertz), which is poorly suited for applications such as nonlinear frequency conversion. The small size of the single-mode core limits the power that can be produced without damage and implies a small filling factor for absorption of the diode light, which occurs over tens of meters. By contrast, diode light absorption can occur in a few meters in multimode fiber. Since high power is present only over a short length of fiber, the threshold for undesired nonlinear processes, such as stimulated Raman scattering, is much higher than in single-mode fiber lasers. The Stokes output is both DLP and narrow-band if the master oscillator is DLP. Alternatively, if image information is present in the pump beam, this information is replicated in the Stokes beam at much higher power. While large amplitude fluctuations are expected if the Stokes field grows from noise, here the simulations suggest that seeding the Stokes field at low power can largely suppress these fluctuations and produce phase locking of the Stokes output with the seed. In order for seeding to be successful, it is necessary to largely eliminate feedback of the Stokes light, which would otherwise overwhelm the low-power seed. If a common pump source is demultiplexed to pump an array of multimode fiber amplifiers, the phase-conjugate Stokes radiation will retrace the paths of the pump beams and, if the Stokes beams are phased correctly and have equal power, the Stokes beams will ideally recombine into a single high-power beam heading back toward the master oscillator (until separated by an optical isolator). The fiber alignment tolerances are much larger than in the situation where one attempts coherent beam combination of single-mode fiber amplifiers in a MOPA configuration. PC makes alignment

Manuscript received November 27, 2000. This work was supported in part by the U.S. Air Force Office of Scientific Research.

The author is with the Air Force Research Laboratory, Directed Energy Directorate, AFRL/DELO, Kirtland AFB, NM 87117-5776 USA.

Publisher Item Identifier S 0018-9197(01)04306-8.

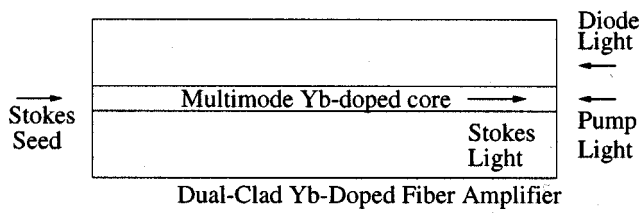


Fig. 1. Schematic diagram of multimode fiber amplifier.

automatic, provided that the master oscillator beams are within the spatial and angular acceptances of the fibers. Correction of thermal distortions is also automatic.

Consider SBS in a fiber of length  $L$ , as shown in Fig. 1. The pump with power  $P_p$  and the diode light with power  $P_d$  enter at  $z = L$  and travel to the left. The Stokes radiation with power  $P_s$  enters as a seed at  $z = 0$  and travels to the right. It is also initiated within the fiber by scattering of the pump from thermal acoustic fluctuations. If the fiber needs to be long compared to the diode light absorption length in order to produce SBS PC, the left part of the fiber can be undoped single-clad fiber with the same core diameter and numerical aperture as the doped fiber. Undoped fiber, besides being less expensive, is not subject to ground-state Yb absorption of  $1.064\text{-}\mu\text{m}$  radiation in the region where the diode light does not penetrate. The advantage of using undoped fiber to enhance SBS generation is lost at very high diode power and brightness, where a total fiber length of a few meters is sufficient.

SBS PC in a waveguide such as a multimode fiber involves an interplay between the effects of diffraction and nonlinearity on highly aberrated and counterpropagating beams. Numerical simulations taking into account the transverse dimensions are difficult. To my knowledge, such simulations [4] have been attempted only subject to simplifying assumptions such as: only one transverse dimension, no time dependence of the field amplitudes, scalar rather than vector fields. Here is proposed a model based on the zeroth-order equations of Hu *et al.* [5]. The Hu equations arise by neglecting terms in the coupled-mode description of SBS in a multimode waveguide which are not phase-matched. The resulting zeroth-order equations do not depend on the transverse coordinates or the normal modes of the fiber, yet are able to account for PC. Chu *et al.* [6] previously reported an analysis of transient SBS PC based on the Hu equations. The equations of my model are generalizations of the Hu equations which include time-dependent dynamics, field attenuation, phonon degrees of freedom, phonon decay, thermal excitation of phonons, and coupling to the  $\text{Yb}^{3+}$  ions and the diode-laser power pumping them.

Suppose that the transverse field distributions of the incident pump and Stokes fields are held fixed. Following the prescription of Hu [5], the pump and Stokes power in terms of complex amplitudes are written as  $p_j(z, t)$  and  $s_j(z, t)$  according to  $P_p = p_j^* p_j$  and  $P_s = s_j^* s_j$ . The Einstein summation convention applies, and  $j = 1$  or  $2$ . The index  $j = 1$  refers to the normalized transverse field distribution and state of polarization  $\mathbf{u}_1(z, \mathbf{r})$  of the pump in the absence of SBS, so that  $p_2(L, t) = 0$ . The phase-conjugate Stokes output power is  $|s_1(L, t)|^2$ , while the nonphase-conjugate (NPC) output power is  $|s_2(L, t)|^2$ . For a

time-independent injected seed, we can take  $s_1(0)$  and  $s_2(0)$  to be real and positive with no loss in generality. Detuning of the SBS gain from resonance can be modeled by letting the phase of  $p_1(L, t)$  be a linear function of time. The distribution  $\mathbf{u}_1(z, \mathbf{r})$  is DLP at  $z = L$ , but aberrated and depolarized at  $z = 0$ . However, it in general has a small overlap with the transverse distribution of the incident seed. This overlap is defined in terms of an inner product, as described below. The amount of overlap depends on the alignment and other characteristics of the seed. After projecting out this overlap, the remainder of the seed orthogonal to  $\mathbf{u}_1(z, \mathbf{r})$  has the normalized distribution  $\mathbf{u}_2(z, \mathbf{r})$ . Note that  $\mathbf{u}_1$  and  $\mathbf{u}_2$  are determined by the incident pump and Stokes fields, and are not normal modes of the fiber. SBS causes mixing of the amplitudes  $p_j$  and  $s_j$ , and, since the gain for the phase-conjugate mode  $\mathbf{u}_1$  is twice that for  $\mathbf{u}_2$ , the fidelity  $\Phi(z) = |s_1(z)|^2 / (|s_1(z)|^2 + |s_2(z)|^2)$  grows from a small value at  $z = 0$  and may approach unity at  $z = L$ . In unseeded SBS, many transverse modes of the Stokes field are excited equally by scattering of the pump from thermal acoustic fluctuations, so that SBS gain causes the phase-conjugate mode to immediately dominate over other modes as  $z$  increases from zero. However, when seeding at low fidelity  $\Phi(0)$ , the  $\mathbf{u}_2$  mode is dominant in the first part of the fiber, and sufficient SBS gain is needed to overcome this dominance and produce good PC at  $z = L$ . Using too strong a seed prevents good PC and can produce unstable operation. On the other hand, too weak a seed leads to increased amplitude fluctuations, lack of phase locking, and dominance of the seed by unavoidable feedback of the Stokes field from the high-power end of the fiber. Seeded PC becomes much easier when  $\Phi(0)$  is not too small.

It has been reported [7] that high-gain SBS in multimode fibers pumped by circularly polarized light produces Stokes light with the same helicity as the pump radiation. This is in contrast to arguments in [8] and measurements for single-mode fibers reported in [9]. The results of [7] suggest that we define an inner product as follows. We write the electric fields in terms of slowly varying envelopes according to  $\mathbf{E}_p = \text{Re}[\mathbf{u}_p(z, \mathbf{r}) \exp(-ik_p z - i\omega_p t)]$  and  $\mathbf{E}_s = \text{Re}[\mathbf{u}_s^*(z, \mathbf{r}) \exp(ik_s z - i\omega_s t)]$ , where  $\mathbf{r}$  is the transverse position. To the extent that  $k_p$  and  $k_s$  are nearly equal,  $u_p$  and  $u_s$  obey the same paraxial wave equation and (in the absence of SBS) the inner product  $\langle u_s | u_p \rangle = \int d^2 r \mathbf{u}_s^* \cdot \mathbf{u}_p$  is conserved. If  $|u_p\rangle = |u_s\rangle$ , the two fields are essentially time reversals of each other. States of circular polarization of opposite helicity are orthogonal.

If the states  $|u_s\rangle$  and  $|u_p\rangle$  are normalized, then (in the absence of SBS)  $\Phi = |\langle u_s | u_p \rangle|^2$ . We can identify  $|u_1\rangle = |u_p\rangle$  and  $|u_2\rangle = (|u_s\rangle - \langle u_p | u_s \rangle |u_p\rangle) / \sqrt{1 - |\langle u_p | u_s \rangle|^2}$ . The effect of SBS PC is to couple the coefficients  $p_1$  and  $s_1$  of  $|u_1\rangle$  with the coefficients  $p_2$  and  $s_2$  of  $|u_2\rangle$  so as to transfer power from the pump to the Stokes field and to make it possible for  $s_1$  to dominate over  $s_2$  by the end of the fiber, because the gain for  $s_1$  is twice as large. This model of SBS PC is independent of the details of the fiber geometry and normal modes, so that the model should be applicable to fibers with elliptical cores or birefringence. However, PC requires highly aberrated beams, which can propagate only in fibers with many modes. PC can be successful only when the incident pump beam is within the spatial

and angular acceptance of the fiber. Enhanced SBS gain for the phase-conjugate field is not expected near  $z = L$  if the incident pump is unaberrated. This is not an important concern, since it appears to be necessary to suppress SBS gain near  $z = L$  (where gain from the  $\text{Yb}^{3+}$  ions is present) in order to obtain stable operation. Inhomogeneous broadening, such as that produced by a longitudinal temperature gradient, can be used to suppress the SBS gain [10].

## II. MATHEMATICAL MODEL

The combined effects of SBS and amplifier gain are explained in terms of the equations

$$\begin{aligned} & \left( \frac{\partial}{\partial z} - \frac{1}{v_g} \frac{\partial}{\partial t} - \frac{\alpha}{2} \right) p_j \\ &= \frac{g}{2A} \rho_{jk}^* s_k - \frac{F}{2} (\sigma_e N_2 - \sigma_a N_1) p_j \end{aligned} \quad (1)$$

$$\begin{aligned} & \left( \frac{\partial}{\partial z} + \frac{1}{v_g} \frac{\partial}{\partial t} + \frac{\alpha}{2} \right) s_j \\ &= \frac{g}{2A} \rho_{kj} p_k + \frac{F}{2} (\sigma_e N_2 - \sigma_a N_1) s_j \end{aligned} \quad (2)$$

$$\begin{aligned} & \left( \frac{\partial}{\partial t} + \frac{\Gamma}{2} [1 + i \Delta(z)] \right) \rho_{jk} \\ &= \frac{\Gamma}{2} (p_j^* s_k + p_m^* s_m \delta_{jk}) + f_{jk} \end{aligned} \quad (3)$$

$$\left( \frac{\partial}{\partial z} - \frac{1}{v_g} \frac{\partial}{\partial t} - \alpha_d \right) P_d = -F_d (\sigma_{ed} N_2 - \sigma_{ad} N_1) P_d \quad (4)$$

$$\begin{aligned} & \frac{\partial N_2}{\partial t} \\ &= -\frac{\lambda_d F_d}{hcA} (\sigma_{ed} N_2 - \sigma_{ad} N_1) P_d - \frac{N_2}{\tau} \\ & \quad - \frac{\lambda F}{hcA} (\sigma_e N_2 - \sigma_a N_1) (p_j^* p_j + s_j^* s_j). \end{aligned} \quad (5)$$

The first three of these equations, if  $F = 0$ , describe SBS PC in a passive fiber. The SBS plane-wave gain in fused silica is  $g = 5 \times 10^{-11} \text{ m/W}$  [11].  $A$  is the fiber core area,  $\alpha$  is an attenuation coefficient (not including attenuation by  $\text{Yb}^{3+}$  ions),  $v_g$  is the group velocity of light in the fiber,  $\Gamma$  is the phonon decay rate,  $\rho_{jk}$  is proportional to the hypersound wave amplitude, and  $f_{jk}$  is a Langevin noise function with the correlation function

$$\langle f_{jk}(z, t) f_{mn}^*(z', t') \rangle = Q \delta_{jm} \delta_{kn} \delta(z - z') \delta(t - t') \quad (6)$$

where [12]

$$Q = \frac{k_B T A \Gamma^2 v_g}{2g v_s}. \quad (7)$$

Here,  $k_B$  is the Boltzmann constant,  $T$  is the temperature, and  $v_s$  is the hypersound velocity.

The function  $\Delta(z) = 2[\omega_p - \omega_s - v_s(k_p + k_s)]/\Gamma$  accounts for inhomogeneous broadening. Both the sound velocity  $v_s$  and the refractive indices depend on temperature, and are functions of  $z$  if there is a longitudinal temperature gradient. Inhomogeneous broadening of SBS gain caused by doping [13]–[15], strain, or temperature inhomogeneities can affect SBS generation. A temperature shift of 2.8 MHz/°C was measured [10] at 1.319  $\mu\text{m}$ .

A shift of 3.5 MHz/°C at 1.064  $\mu\text{m}$  seems plausible. Applying heat or strain near  $z = L$  can be expected to shift the Stokes resonance so that Stokes radiation generated near  $z = 0$  experiences little SBS gain near  $z = L$ . Such heat or strain is a likely by-product of high-power operation. Since my simulations including amplifier gain usually predict unstable operation unless the SBS interaction is suppressed at the high-power end of the fiber, inhomogeneous broadening appears to be a useful effect. Constant  $\Delta$  describes uniform detuning from resonance, and can be transformed out of the equations by supposing that  $p_j$  and  $\rho_{jk}^*$  have phase oscillations  $\exp[(i\Gamma \Delta/2)(t + z/v_g)]$ . In numerical simulations, it is sufficient to impart these oscillations to  $p_1(L, t)$ .

If we neglect the noise functions  $f_{jk}$  and set  $\alpha = 0$ , the phonon field can be eliminated in the steady-state and the equations for SBS in a passive fiber take the form

$$\frac{dp_j}{dz} = \frac{g}{2A(1 - i\Delta)} (s_k^* s_k p_j + s_k^* p_k s_j) \quad (8)$$

$$\frac{ds_j}{dz} = \frac{g}{2A(1 + i\Delta)} (p_k^* p_k s_j + p_k^* s_k p_j). \quad (9)$$

These equations imply an integration constant  $p_j^* p_j - s_j^* s_j = C$ , representing conservation of energy. If  $\Delta = 0$ ,  $p_j$  and  $s_j$  can be chosen real without loss of generality and (8) and (9) are equivalent to the zeroth-order equations of Hu for SBS phase conjugation [5]. Analytic solutions of the Hu equations can be obtained [5], but no general analysis of the stability of these solutions is presently available.

Analytic solutions for nonzero  $\Delta$  seem to be possible only in special cases. A case of some importance is when  $p_2$  and  $s_2$  are identically zero. This case is a good approximate description for the desirable situation where  $s_2$  does not grow large enough at  $z = L$  to play a significant role in depleting the pump and where the fidelity  $\Phi(L)$  is near unity. If we set  $p_1 = P_p^{1/2} e^{i\phi_p}$  and  $s_1 = P_s^{1/2} e^{i\phi_s}$ , we easily obtain the solutions

$$P_p(z) = \frac{CP_p(0)}{P_p(0) - P_s(0)e^\eta} \quad (10)$$

$$P_s(z) = \frac{CP_s(0)e^\eta}{P_p(0) - P_s(0)e^\eta} \quad (11)$$

$$\eta = \frac{2gC}{A} \int_0^z dz' \frac{1}{1 + \Delta^2(z')}. \quad (12)$$

The phases can then be obtained by integration of

$$\frac{d\phi_p}{dz} = \frac{g}{A} \frac{\Delta(z)}{1 + \Delta^2(z)} P_s(z) \quad (13)$$

$$\frac{d\phi_s}{dz} = -\frac{g}{A} \frac{\Delta(z)}{1 + \Delta^2(z)} P_p(z). \quad (14)$$

The gain in (12) is twice as large as for plane waves, as is expected for phase-conjugate SBS amplification. A characteristic power scale for the SBS gain is  $2A/gL$ , which implies that high-power devices can be much shorter than the fibers used by [1] and [2], [24]. Detuning from resonance reduces the gain and also produces a dynamical phase shift of the output Stokes light

relative to the incident seed. If thermal noise is taken into account, phase locking is limited to small detuning because the SBS gain on resonance is higher than at the seed frequency. However, appreciable phase shifts can occur within the locking range.

In situations where  $s_2$  gets large enough to contribute significantly to pump depletion, the numerical calculations here sometimes predict unstable behavior. Instability can occur even in the absence of amplifier gain. It typically occurs when the seed power is too high or  $\Phi(0)$  is too small, so that the higher gain of  $s_1$  is not sufficient for  $s_1$  to win out against  $s_2$  by the end of the fiber. The instability can take various forms, including limit-cycle oscillations, possibly chaotic fluctuations, and regimes where the fields remain nearly constant over many fiber transit times  $L/v_g$ , but then undergo a “burp” before returning to quiescence. These dynamical effects are in addition to, and somewhat masked by, stochastic thermal fluctuations, which are present also in stable regimes. Unstable dynamics for SBS in the presence of feedback was predicted long ago [16], but no feedback is included in my model.

Now let us consider SBS PC in an active fiber amplifier, as described by (1)–(5). The diode power is injected at  $z = L$ .  $N_1$  and  $N_2$  are the populations of the lower and upper manifolds of the  $\text{Yb}^{3+}$  ion with sum  $N = N_1 + N_2$  which is constant (or more generally a function of  $z$ ),  $\sigma_e$  and  $\sigma_a$  are emission and absorption cross sections for the pump and Stokes fields,  $\sigma_{ed}$  and  $\sigma_{ad}$  are emission and absorption cross sections for the diode field,  $\tau$  is the uppermanifold lifetime,  $\lambda$  is the pump wavelength (nearly equal to the Stokes wavelength),  $\lambda_d$  is the diode wavelength,  $\Gamma$  is the phonon decay rate,  $\alpha_d$  characterizes attenuation of the diode field (other than by  $\text{Yb}^{3+}$  ions), and  $F$  and  $F_d$  are filling factors.  $F$  is the ratio of the effective area receiving amplifier gain to the area  $A$  of optical confinement of the pump and Stokes light.  $F_d$  is the ratio of this effective area to the area of the inner cladding which confines the diode light. The larger filling factor  $F_d$  of multimode fibers as compared to single-mode fibers means that diode light absorption occurs over a shorter length.

As default parameters for an example which will be discussed below, consider a fiber amplifier with a core diameter of 50  $\mu\text{m}$  and length  $L = 5$  m. The diode power is 1570 W ( $gL P_d(L)/2A = 100$ ) at  $\lambda_d = 0.975$   $\mu\text{m}$  with  $F_d = 0.053$ . These numbers presume future improvements in the brightness of diode-laser arrays, such as might be obtainable by geometrical transformations [17], [18]. The incident pump power is 157 mW at  $\lambda = 1.064$   $\mu\text{m}$ . The seed Stokes power is 0.43 mW with  $\Phi(0) = 1\%$  in the phase-conjugate mode and down-shifted from the pump by the Stokes shift of about 15 GHz. Both the pump and Stokes radiation are assumed to be monochromatic. The phonon decay rate is  $\Gamma/2\pi = 36$  MHz. Other parameters in the simulation are light group velocity  $v_g = 2 \times 10^8$  m/sec, sound speed  $v_s = 5.96$  km/s,  $\alpha L = 0.1$ ,  $\alpha_d = 0$ ,  $F = 0.82$ , and  $N = 1.0 \times 10^{26}$   $\text{m}^{-3}$ . The values of  $\sigma_e = 3.0 \times 10^{-25}$   $\text{m}^2$ ,  $\sigma_a = 6.0 \times 10^{-27}$   $\text{m}^2$ ,  $\sigma_{ed} = \sigma_{ad} = 2.5 \times 10^{-24}$   $\text{m}^2$ , and  $\tau = 0.84$  ms are taken from [19] and [20]. The fiber has inhomogeneous broadening over the last 1.5 m, given by a linear ramp in  $\Delta(z)$  from zero at  $z = 3.5$  m up to 12 (corresponding to 216 MHz or about 62°C) at  $z = L$ . There is an additional detuning of 4 MHz over

the whole fiber shifted from resonance in the same direction as the ramp.

Even apart from SBS gain, the Yb amplifier could produce a small-signal single-pass gain at the pump or Stokes frequencies on the order of  $\exp(FNL\sigma_e) = \exp(123)$  in the limit that the diode light completely inverts the medium. Even when enough diode power is available, this huge gain cannot be approached because unavoidable feedback and amplified spontaneous emission (effects not included in the current modeling) first cause the fiber to dump power. This means that pump and Stokes output cannot be turned off by turning off the incident pump and Stokes beams. Instead, the upper manifold of  $\text{Yb}^{3+}$  levels becomes appreciably populated only near the high-power end of the fiber, and the diode field is strongly attenuated before reaching  $z = 0$ . The combined SBS and amplifier gain for regimes of interest in this paper is less than  $P_d(L)/P_s(0)$ , which equals  $3.7 \times 10^6$  for the default parameters. Eliminating feedback to below the level of the incident seed is still challenging. The situation becomes more favorable if  $\Phi(0)$  is larger than 1%, so that a stronger Stokes seed can be used without destroying PC. Under conditions of high SBS reflectivity, the single-pass, strong-signal gain of the amplifier (apart from SBS gain) is no more than a few times  $\sqrt{P_d(L)/P_p(L)} = 100$ . For this reason, Brillouin scattering from thermal phonons is expected to dominate over spontaneous emission from excited  $\text{Yb}^{3+}$ . This justifies my neglect of the latter effect.

### III. NUMERICAL SOLUTIONS

The numerical solutions are obtained using second-order Runge–Kutta integration along the characteristics of the partial differential equations. The fields are calculated at 201 space points, and the ratio of space intervals to time intervals is  $v_g$ . Thermal noise  $f_{jk}$  is generated by independent Gaussian random variables at each space-time point. Most of the simulations reported here reach steady state, except for the stochastic effects of thermal fluctuations. Since the population  $N_2$  equilibrates very slowly compared to the fiber transit time, it speeds convergence to multiply the right side of (5) by a factor larger than unity (but too large a factor can cause instability) while the device is equilibrating. Partial bleaching of pump and Stokes absorption near the low-power end of the fiber is particularly slow.

Fig. 2 shows the quasi-steady-state amplitudes  $|p_1|$ ,  $|s_1|$ ,  $|p_2|$ ,  $|s_2|$ , and  $\sqrt{P_d}$ , as well as the normalized uppermanifold population  $N_2/N$ , as a function of position for the default parameters given above. The output is  $|s_1(L)|^2 \approx 1235$  W,  $|s_2(L)|^2 \approx 112$  W, and  $|p_1(0)|^2 \approx 64$  W. The diode light is completely depleted. The phase of  $s_1(L, t)$  fluctuates within a range of about 4°.  $N_2$  has a maximum at about 0.6 m before the end of the fiber and decreases close to  $z = L$  because of energy extraction by the Stokes field. Amplifier gain is limited to the last meter of fiber. Since the Stokes power is high only over a short distance near the end of the fiber where SBS has been frustrated by inhomogeneous broadening, generation of second-order Stokes radiation traveling toward  $z = 0$  should not be a problem.

The temporal evolution which culminates in the fields shown in Fig. 2 is initiated with fields which are constant in  $z$  and

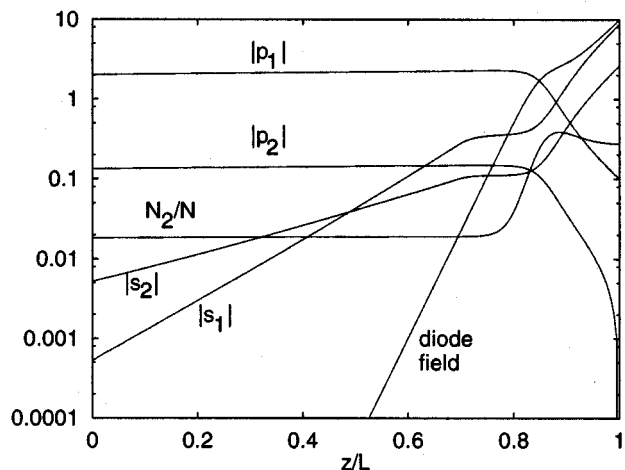


Fig. 2. Field moduli  $|p_1|$ ,  $|p_2|$ ,  $|s_1|$ ,  $|s_2|$ , and  $\sqrt{P_d}$ , as well as the normalized uppermanifold population  $N_2/N$ , are shown as a function of  $z$  in the quasisteady state for the default parameters of the modeling. The fields are given in units of  $\sqrt{2A/gL}$ , where  $2A/gL = 15.7$  W.

with  $N_2 = \rho_{jk} = 0$ . Spatial attenuation of the diode field occurs within a single pass. The pump and Stokes fields exhibit smaller attenuation due to  $\sigma_a$  and  $\alpha$ .  $N_2$  and  $p_1$  gradually increase in time, with  $N_2$  peaked at  $z = L$ . The Stokes fields  $s_1$  and  $s_2$  increase with  $z$  near  $z = L$  because of amplifier gain, but not at first to significant levels. When  $p_1$  has grown sufficiently, Brillouin scattering from thermal phonons in some cases may temporarily disrupt phase locking of  $s_1(L, t)$  with the seed. Phase locking is recovered as the SBS process saturates, and phase conjugation occurs as  $s_1$  dominates  $s_2$  at the high-power end of the fiber. Saturation occurs smoothly, without large spikes or oscillations in the Stokes output. The maximum in  $N_2$  then shifts to the interior of the fiber. Partial bleaching of ground-state absorption of the pump and Stokes light at the low-power end of the fiber occurs over many transit times and typically reduces  $|s_1(L, t)|^2$  slightly. It is essential to frustrate SBS at the high-power end of the fiber (here accomplished by a linear ramp in  $\Delta$ ). Otherwise, unstable operation occurs.

Figs. 3–10 show the effects of stepping a parameter of the device through a series of values. Following a sudden shift in the value of the chosen parameter, the device relaxes back toward a new steady state. Figs. 3 and 4 show the effect of shifting the pump frequency by 1 MHz at time intervals of  $30L/v_g$ . The frequency detunings from resonance with the low-power part of the fiber having  $\Delta = 0$  are shown on the top scale, with positive values indicating a shift from resonance in the same direction as that produced by the ramp in  $\Delta$  at the high-power end of the fiber. Negative or too large positive detuning produces coherent oscillations. In this simulation, an additional 1-MHz detuning (not shown) caused loss of phase locking. The exiting pump power  $P_p(0)$  (bottom curve in Fig. 3) is relatively insensitive to pump frequency or other parameters. The phase of  $s_1(L, t)$  (Fig. 4) does shift with pump frequency (or other parameters).

Fig. 5 shows the effect of increasing the seed power by a factor of 4 after each time interval  $30L/v_g$ , starting with the default seed power and keeping  $\Phi(0) = 0.01$ . Too strong a seed disrupts phase conjugation, since there is insufficient SBS gain

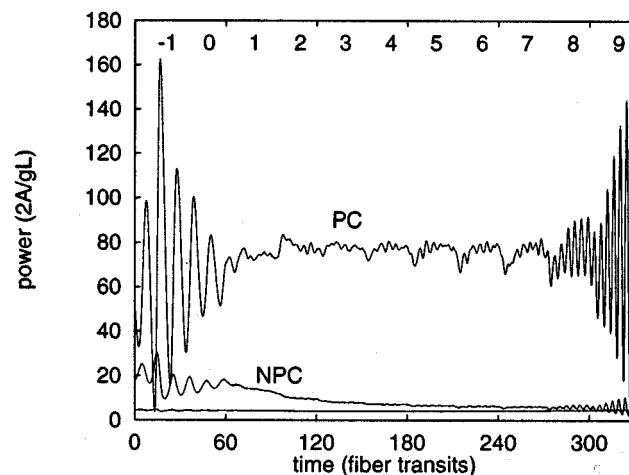


Fig. 3. Phase-conjugate power  $|s_1(L, t)|^2$  (upper curve),  $|s_2(L, t)|^2$  (middle curve), and exiting pump  $P_p(0, t)$  (bottom curve) are shown for a situation where the pump frequency jumps by 1 MHz (upper scale) after time intervals  $30L/v_g = 750$  ns. Coherent oscillations occur at excessive detuning.

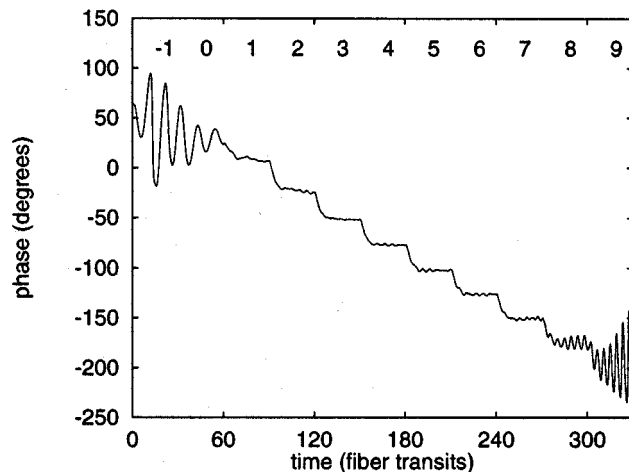


Fig. 4. Phase of  $s_1(L, t)$  as the pump frequency is shifted in steps of 1 MHz.

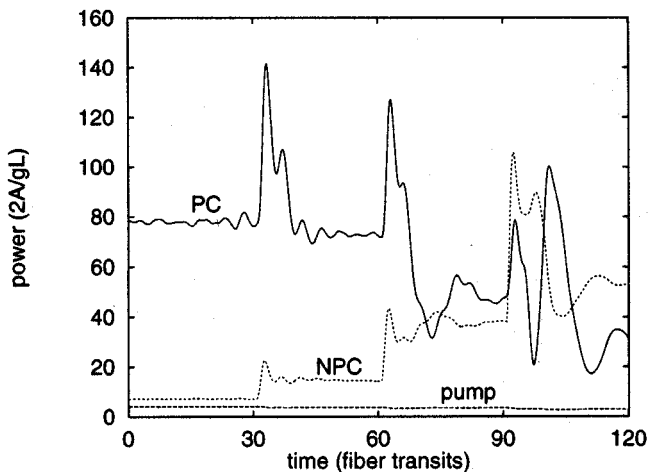


Fig. 5.  $|s_1(L, t)|^2$  (PC),  $|s_2(L, t)|^2$  (NPC), and  $P_p(0, t)$  (pump) are shown for a situation where the seed power  $P_s(0, t)$  is stepped up by a factor of four after each time interval  $30L/v_g$ , starting with the default value. Too strong a seed leads to poor phase-conjugation fidelity.

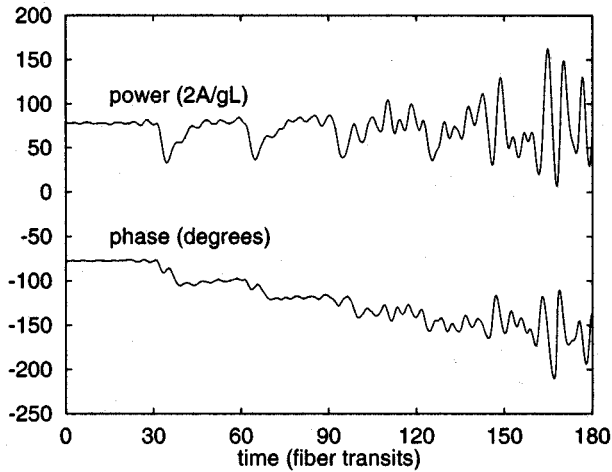


Fig. 6.  $|s_1(L, t)|^2$  and the phase of  $s_1(L, t)$  are shown for a situation where the seed power  $P_s(0, t)$  is stepped down by a factor of four after each time interval  $30L/v_g$ , starting with the default value. Too weak a seed leads to increased fluctuations, though the average power is not appreciably affected and the PC fidelity remains high.

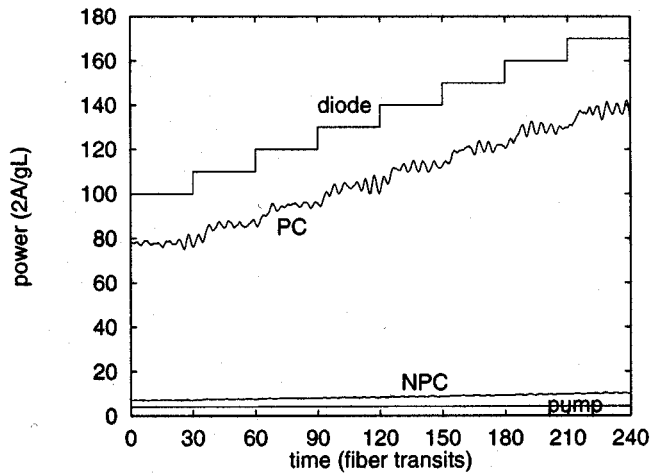


Fig. 7. The effect of stepping up  $P_d(L, t)$  (diode), starting with the default value. The other curves show  $|s_1(L, t)|^2$  (PC),  $|s_2(L, t)|^2$  (NPC), and  $P_p(0, t)$  (pump).

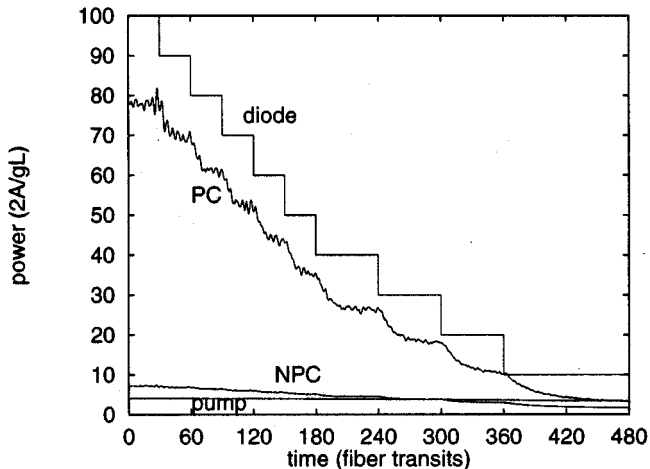


Fig. 8. The effect of stepping down the diode power  $P_d(L, t)$ , starting with the default value. Efficiency and PC fidelity both decrease at very low diode power.

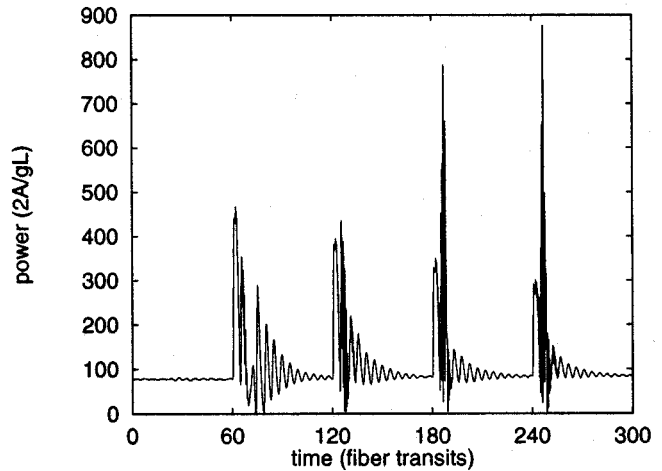


Fig. 9. Phase-conjugate power  $|s_1(L, t)|^2$  is shown as a function of time for a situation where the pump power  $P_p(L, t)$  is doubled after each interval  $60L/v_g$ , starting with the default value. Large transient power spikes occur at the switching times. Relaxation occurs to a Stokes power which increases with pump power.

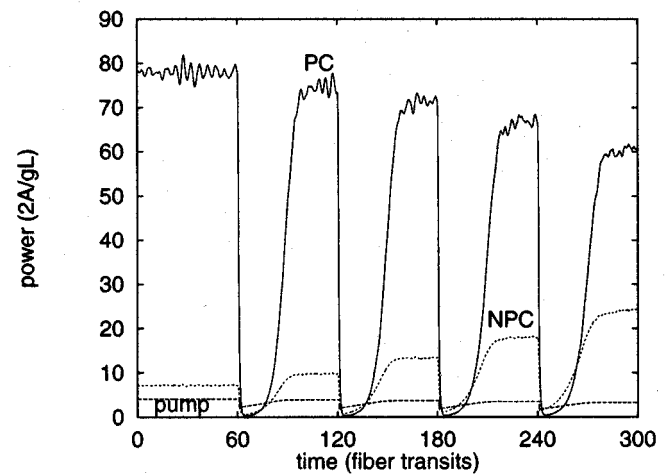


Fig. 10. Pump power  $P_p(L, t)$  is halved after each interval  $60L/v_g$ , starting with the default value. Transients occur during which SBS switches off and then recovers. Too low a pump power results in poor fidelity, as  $|s_2(L, t)|^2$  (NPC) becomes comparable to  $|s_1(L, t)|^2$  (PC). The bottom curve shows  $P_p(0, t)$ .

with a strong seed for  $s_1$  to dominate over  $s_2$  at the end of the fiber. Fig. 6 shows the effect of decreasing the seed power by a factor of four after each time interval  $30L/v_g$ , starting with the default seed power. This results in increased fluctuations in the power and phase of  $s_1(L, t)$ , as the role of thermal noise in initiating SBS becomes more prominent. In practice, feedback (not included here) would also become more significant.

Figs. 7 and 8 show the effect of ramping up and down the diode power, starting from the default value. I ascribe the lack of strong transients to the slow time response of  $N_2$  to changes in the diode power. The wavelength ratio  $\lambda_d/\lambda = 92\%$  is an upper limit on the device efficiency, whereas the numerical results at the default diode power give a total conversion to pump and Stokes power of 86%, with about 79% conversion to phase-conjugate Stokes power. After the diode power has been reduced to 10% of the default value, spontaneous decay of ions in the upper manifold reduces the total conversion to pump and Stokes

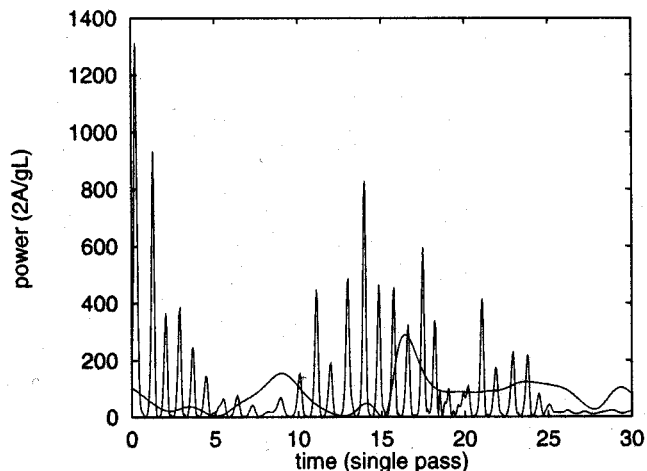


Fig. 11. Phase-conjugate power  $|s_1(L, t)|^2$  for unseeded SBS with (smooth curve) and without (spiky curve) inhomogeneous broadening to suppress SBS at the high-power end of the fiber.

radiation to about 50%, with only 33% being phase-conjugate Stokes radiation. At this diode power level, a longer fiber would enhance the SBS gain and improve the efficiency.

Figs. 9 and 10 show the effect of ramping up and down the pump power  $P_p(L, t)$  by a factor of two every time interval  $60L/v_g$ , starting from the default value. Stepping up the pump power causes a strong spike in the power  $|s_1(L, t)|^2$ , followed by a small increase in the steady-state power. A transient numerical anomaly (saw-tooth oscillations in  $z$ ) is also found, as a result of suddenly increasing the pump power. Stepping down the pump power causes the Stokes output to shut off and then recover. Making the pump power too low destroys phase conjugation, though the total Stokes power stays high. In the limit of zero pump there is no SBS, but the Stokes seed can nevertheless be amplified to extract the energy stored in the  $\text{Yb}^{3+}$  ions. To avoid the large fluctuations shown in these figures, it is important to use a master oscillator without large short-term amplitude fluctuations.

Fig. 11 shows typical time dependence of  $|s_1(L, t)|^2$  for unseeded SBS. The smoother curve with low peaks is with the default ramp in  $\Delta$ . The curve with high sharp spikes is for  $\Delta = 0$ , which illustrates the effect of dynamical instability. This effect causes the peak Stokes power to occasionally exceed the diode power by an order of magnitude. Dynamical instability also causes  $P_p(0, t)$  to fluctuate strongly. For this example, the time between spikes is short compared to the round-trip time  $2L/v_g$ . The maximum possible average power can be reduced by spiking because optical damage can occur at high peak power. However, spiking can enhance the efficiency for nonlinear frequency conversion processes, such as second-harmonic generation. The fidelity  $\Phi(L)$  is excellent for both regimes illustrated in Fig. 11. Seeding is ineffective in the unstable regime.

The above simulations illustrate the potential of SBS PC for generating very high power. However, SBS PC can be used at moderate power by increasing the fiber length inversely with the power level. Excessive ground-state absorption of pump and Stokes radiation at the low-power end of a long fiber can be

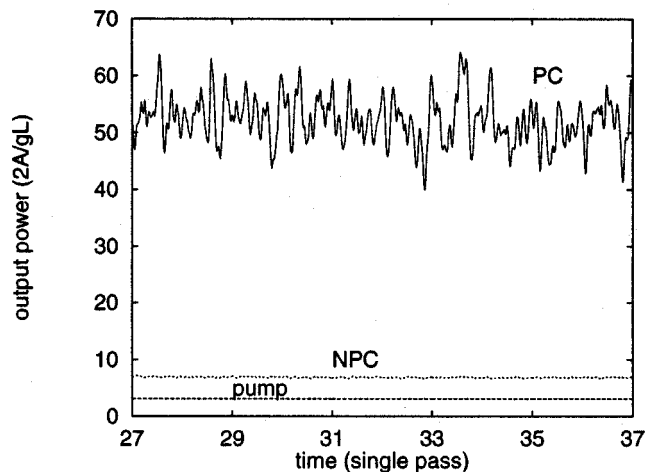


Fig. 12. Quasi-steady-state output power for a fiber of length  $L = 200$  m. The input diode, pump, and Stokes seed power, scaled inversely to  $L$ , are 2.5% of the power. For the default parameters of the high-power example.

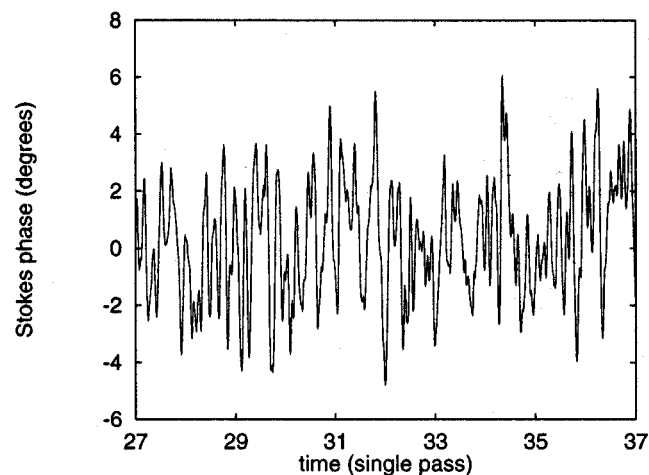


Fig. 13. Quasisteady-state phase of  $s_1(L, t)$  for a fiber of length  $L = 200$  m.

avoided either by decreasing  $N$  uniformly along the fiber or by coupling a short length of Yb-doped fiber to a longer section of passive fiber. Good results in simulations were obtained using either method with a fiber of length  $L = 20$  m and  $P_d(L) = 392$  W. With the first method,  $N$  must be kept large enough so that the diode light is absorbed in the short fraction of the fiber length where SBS is suppressed by inhomogeneous broadening. Otherwise, instability occurs. The second method avoids the expense of using a long length of custom fiber, but imperfect coupling could increase undesirable feedback of Stokes radiation to the low-power end of the fiber.

The simulations have demonstrated high efficiency and phase locking for fibers as long as 200 m (the final 5 m doped with  $\text{Yb}^{3+}$ ) with  $P_d(L) = 39$  W. Figs. 12 and 13 show the quasisteady-state output power and the phase of  $s_1(L, t)$  for such a case. Parameters for this example are  $N = 0.3 \times 10^{26} \text{ m}^{-3}$ ,  $\alpha L = 0.1$ , and  $\Delta(L) = 15$ . The linear ramp in  $\Delta$  is over the 5 m of doped fiber. SBS in the passive fiber is on resonance. Other fiber parameters are the same as for the previous high-power example. The power of all input beams is scaled inversely to  $L$ , as

compared to the high-power example. This regime is well suited for initial experimentation. Simulations are very slow for such long fibers, since a large number of spatial grid points must be used to resolve the fields in the short amplifier section of the fiber. Relative intensity and phase fluctuations are somewhat larger than at higher power. The efficiency  $|s_1(L)|^2/P_d(L) \approx 55\%$  is lower than at higher power. This is because spontaneous decay of ions in the upper manifold is relatively more likely at low power. The phonon lifetime and the fiber transit time are of the same order of magnitude for the high-power example, whereas the phonon lifetime is much shorter than the fiber transit time for the low-power example ( $\Gamma L/v_g = 225$ ). The phonon lifetime determines the SBS gain bandwidth and influences the phase-locking bandwidth. The Stokes intensity fluctuations have features which last for many phonon lifetimes. They, thus, seem analogous to oscillations of a particle trapped in a potential well and undergoing Brownian motion. For the low-power example, the ramp in  $\Delta$  is not required in order to avoid dynamical instability. However, the ramp improves the efficiency and PC fidelity and reduces the phase fluctuations in  $s_1(L, t)$ .

#### IV. DISCUSSION

The model presented here incorporates many features expected to be important for multimode fiber amplifiers utilizing SBS PC, and numerical solutions can be readily obtained. Nevertheless, the model is only an approximate description of a very complex process, nor has it yet been compared with experiments. Some features of the model seem unsatisfactory and in need of improvement. For example, it is not clear how to estimate or to measure the fidelity  $\Phi(0)$  at the low-power end of the fiber. If the pump power becomes distributed randomly over all the fiber modes as a result of propagating through the fiber, one would expect  $\Phi(0)$  to scale inversely with the number of modes, that is, inversely with  $A$ . This could prevent seeding of PC when  $A$  is too large. On the other hand, possibly a DLP incident pump which is well within the spatial and angular acceptance of the fiber remains distributed over a relatively small number of fiber modes. Optical transport within a multimode fiber has been described as a power-diffusion process [21] in which the modal distribution spreads, this spreading being limited by increased attenuation of the higher-order modes. In this process, information is lost about the initial spatial distribution of the pump. Thus, PC at the low-power end of the fiber is providing increased gain, not to the incident pump distribution, but to the relaxed pump distribution. Such loss of information also occurs if the low-power end of the fiber is tapered, which has been done to enhance SBS PC at low power [22].

The simulations presented in this paper are for situations where (except for sudden jumps) the incident pump and Stokes seed are monochromatic. If the transverse distributions are fixed, one can calculate more general time dependence within the framework of this model. If the transverse distributions vary with time, it may be appropriate to extend the model by coupling more than two modal dimensions. PC will be inhibited

if the pump field is incoherent to the extent that its transverse distribution changes appreciably within a fiber transit time. Variations of  $\Phi(0)$  on a slower time scale could possibly cause intermittent loss of phase locking.

The issue of polarization restoration associated with SBS PC in multimode fibers has been studied experimentally for the case of linear polarization [1], [2], [24], but not to the author's knowledge for circular or elliptical polarization. The fiber used by [7] supported only a few modes, and so was not suitable for PC. Since axially symmetric multimode fibers preserve circular polarization with a high degree of accuracy [23], it is of particular interest to study PC for this case.

In conclusion, a model of SBS PC in multimode Yb-doped fiber amplifiers has been presented and have been described numerical solutions based on this model. My model predicts that low-power seeding of the Stokes field can produce phase locking to the high-power phase-conjugated Stokes output over a bandwidth of a few megahertz and help suppress its intensity fluctuations. SBS dynamical instability can occur, even in passive fiber without feedback. It is necessary to segregate the SBS gain and amplifier gain in different sections of the fiber to prevent instability. SBS at the high-power end of the fiber can be suppressed by inhomogeneous broadening. Amplifier gain is restricted to this region by the short length for absorption of diode light. Passive fiber can be used for the SBS section. This is advantageous at low power, where a long SBS section is needed. Power scaling to greater than 1 kW of DLP output per fiber amplifier should be possible. Coherent combination of beams from an array of fiber amplifiers phase-locked to a common Stokes seed may also be possible. PC should be able to correct thermal aberrations at high power, provided that injection of light from the master oscillator into the fiber is not inhibited. The best choices for core and cladding areas and fiber length depend on the brightness of the diode light. Generally, lower brightness necessitates using larger area and longer fibers to reach a given power level.

#### REFERENCES

- [1] V. I. Kovalev and R. G. Harrison, "Diffraction limited output from a CW Nd:YAG master oscillator/power amplifier with fiber phase conjugate SBS mirror," *Opt. Commun.*, vol. 166, pp. 89–93, 1999.
- [2] H. J. Eichler, J. Kunde, and B. Liu, "Quartz fiber phase conjugators with high fidelity and reflectivity," *Opt. Commun.*, vol. 139, pp. 327–334, 1997.
- [3] G. J. Cowle and D. Y. Stepanov, "Hybrid Brillouin/erbium fiber laser," *Opt. Lett.*, vol. 21, pp. 1250–1252, 1996.
- [4] R. H. Lehmborg, "Numerical study of phase conjugation in stimulated Brillouin scattering from an optical waveguide," *J. Opt. Soc. Amer.*, vol. 73, pp. 558–566, 1983.
- [5] P. H. Hu, J. A. Goldstone, and S. S. Ma, "Theoretical study of phase conjugation in stimulated Brillouin scattering," *J. Opt. Soc. Amer. B*, vol. 6, pp. 1813–1822, 1989.
- [6] R. Chu, M. Kanefsky, and J. Falk, "Transient phase conjugation by stimulated Brillouin scattering: Numerical analysis of zero-order solutions," *J. Opt. Soc. Amer. B*, vol. 11, pp. 331–338, 1994.
- [7] B. C. Rodgers, T. H. Russell, and W. B. Roh, "Laser beam combining and cleanup by stimulated Brillouin scattering in a multimode optical fiber," *Opt. Lett.*, vol. 24, pp. 1124–1126, 1999.
- [8] B. Y. Zel'dovich, N. F. Pilipetsky, and V. V. Shkunov, *Principles of Phase Conjugation*. Berlin, Germany: Springer-Verlag, 1985.
- [9] M. O. van Deventer and A. J. Boot, "Polarization properties of stimulated Brillouin scattering in single-mode fibers," *J. Lightwave Technol.*, vol. 12, pp. 585–590, 1994.



- [10] Y. Imai and N. Shimada, "Dependence of stimulated Brillouin scattering on temperature distribution in polarization-maintaining fibers," *IEEE Photon. Technol. Lett.*, vol. 5, pp. 1335–1337, 1993.
- [11] G. P. Agrawal, *Nonlinear Fiber Optics*, 2nd ed. San Diego, CA: Academic, 1995.
- [12] R. W. Boyd, K. Rzażwski, and P. Narum, "Noise initiation of stimulated Brillouin scattering," *Phys. Rev. A*, vol. 42, pp. 5514–5521, 1990.
- [13] X. P. Mao, R. W. Tkach, A. R. Chraplyvy, R. M. Jopson, and R. M. Derosier, "Stimulated Brillouin threshold dependence on fiber type and uniformity," *IEEE Photon. Technol. Lett.*, vol. 4, pp. 66–69, 1992.
- [14] K. Shiraki, M. Ohashi, and M. Tateda, "SBS threshold of a fiber with a Brillouin frequency shift distribution," *J. Lightwave Technol.*, vol. 14, pp. 50–57, 1996.
- [15] —, "Performance of strain-free stimulated Brillouin scattering suppression fiber," *J. Lightwave Technol.*, vol. 14, pp. 549–554, 1996.
- [16] I. Bar-Joseph, A. A. Friesem, E. Lichtman, and R. G. Waarts, "Steady and relaxation oscillations of stimulated Brillouin scattering in single-mode optical fibers," *J. Opt. Soc. Amer. B*, vol. 2, pp. 1606–1611, 1985.
- [17] T. Y. Fan, "Efficient coupling of multiple diode laser arrays to an optical fiber by geometric multiplexing," *Appl. Opt.*, vol. 30, pp. 630–632, 1991.
- [18] J. R. Leger and W. C. Goetsos, "Geometrical transformation of linear diode-laser arrays for longitudinal pumping of solid-state lasers," *IEEE J. Quantum Electron.*, vol. 28, pp. 1088–1100, 1992.
- [19] H. M. Pask, R. J. Carman, D. C. Hanna, A. C. Tropper, C. J. Mackechnie, P. R. Barber, and J. M. Dawes, "Ytterbium-doped silica fiber lasers: Versatile sources for the 1–1.2 $\mu$ m region," *IEEE J. Select. Topics Quantum Electron.*, vol. 1, pp. 2–13, 1995.
- [20] R. Paschotta, D. C. Hanna, P. De Natale, G. Modugno, M. Inguscio, and P. Laporta, "Power amplifier for 1083 nm using ytterbium doped fiber," *Opt. Commun.*, vol. 136, pp. 243–246, 1997.
- [21] D. Gloge, "Optical power flow in multimode fibers," *Bell System Tech. J.*, vol. 51, pp. 1767–1783, 1972.
- [22] A. Heuer and R. Menzel, "Phase-conjugating stimulated Brillouin scattering mirror for low powers and reflectivities above 90% in an internally tapered optical fiber," *Opt. Lett.*, vol. 23, pp. 834–836, 1998.
- [23] A. Y. Savchenko and B. Y. Zel'dovich, "Wave propagation in a guiding structure: one step beyond the paraxial approximation," *J. Opt. Soc. Amer. B*, vol. 13, pp. 273–281, 1996.
- [24] A. Mocofanescu, *Presentation*, AFRL/DELO, May 5, 2000.

**Gerald T. Moore** was born in Troy, NY, in 1943. He received the B.S. degree in physics from Rensselaer Polytechnic Institute, Troy, NY, in 1965 and the Ph.D. degree in physics from Brandeis University, Waltham, MA, in 1969.

After eight years at the University of Arizona, he joined the University of New Mexico, Albuquerque, in 1980, where he became a Research Associate Professor with the Center for Advanced Studies. His research since 1989 was carried out at Kirtland AFB, Albuquerque, NM. He began his current position as a Research Physicist with the Air Force Research Laboratory in 1999. His research background includes work on quantum field theory with time-dependent boundary conditions, free-electron lasers, laser accelerators, unstable laser resonators, and the modeling of devices for nonlinear optical frequency conversion.